Empirical estimation of metal powder bed fusion technological improvement rate

Progress in Additive Manufacturing
https://doi.org/10.1007/s40964-024-00813-8

FULL RESEARCH ARTICLE

Empirical estimation of metal powder bed fusion technological improvement rate

António Alves de Campos[1] · Bruna Torres Ferreira[1] · Afonso Gonçalves[1] · Marco Leite[1] · Inês Ribeiro[1] · Christopher L. Magee[2] · Elsa Henriques[1]

Received: 2 March 2024 / Accepted: 17 September 2024

Abstract
This study empirically estimates the technological improvement rate (TIR) of metal powder bed fusion (PBF) technology, widely used in aerospace, automotive, and medical industries. PBF's continuous long-term adoption growth is driven by its ability to enhance manufacturing efficiency in terms of time and raw material use, as well as its capability to produce high-quality, high-strength, complex-shaped parts. Measuring the technological development of PBF is crucial as itis enlarging its application domain and is increasingly considered a viable alternative to traditional manufacturing technologies across a broader range of applications. We resorted to the literature to collect information and assess which technical parameters are most relevant to measure the capabilities of PBF. With those, we established an ideal functional performance metric (FPM) capable of comprehensively assessing PBF's technological performance improvement. Considering all available data sources and PBF machines ever made commercially available, a data set of technical parameters was constructed. This was followed by a data curation process focusing on data availability and reliability. The resultant practical FPM was used to estimate the TIR of PBF technology. By employing regression analysis, we estimate a yearly improvement of 26.8%. This empirical rate comes as a more accurate and reliable substitute to the previously indirectly estimated patent-derived rate of 33.3%. Our findings underscore PBF's capability of keeping pace with its growing significance and wider industrial applications. The results of this study provide a key metric for those in the industry and research, confirming the rapid performance growth and establishing a standard for future industrial uses.

Keywords Powder bed fusion · Additive manufacturing · Manufacturing technology · Technological improvement rates · Technological performance estimation

1 Introduction

Additive manufacturing (AM) involves building 3D solid objects by layering material, based on designs from computer-aided design (CAD) models [1–3], offering a significant shift from traditional manufacturing methods such as milling, grinding, stamping, injection molding, and casting due to its reduced manufacturing steps and enhanced resource efficiency [1–3]. The 2023 Wohlers Report indicates a global increase of 18.3% in AM products and services, continuing the trend of double-digit revenue growth in the AM industry observed in the last three decades [4]. Among AM technologies, metal PBF technological family stands out for its ability to produce high-value, precisely controlled components across various metal alloys [5, 6]. Metal PBF technologies rely on the deposition of a thin layer of powder onto a substrate plate or onto the previously deposited layer and subsequently selectively melting or sintering it using a laser—laser powder bed fusion (PBF–LB/M), or an electron beam—electron beam melting powder bed fusion (PBF–EB/M), following the design data provided by CAD model [7–11].

The development of metal PBF technology, henceforth denoted simply by PBF, began in the mid-1980 at University of Texas aiming to streamline the lengthy process of creating new parts. Early systems significantly reduced the need for manual tool path planning and fixtures, leading

✉ António Alves de Campos
antonio.campos@tecnico.ulisboa.pt

[1] IDMEC, Instituto Superior Técnico, Universidade de Lisboa, Lisbon, Portugal

[2] Massachusetts Institute of Technology, Cambridge, MA 02139, USA

Published online: 22 October 2024

to the emergence of commercial machines such as DTM 125 and SinterStation 2000. Over time, PBF evolved from prototyping to manufacturing functional parts, supported by advancements in materials and machine design, significantly impacting industries by enabling the production of complex geometries and the use of diverse materials, including metals. This period of rapid development highlighted PBF's role in transforming manufacturing processes from traditional methods to additive manufacturing, marking its growth as a key technology for various sectors [12]. Currently, PBF is used in several highly technological sectors such as the medical, aerospace, and automotive industries where tailored designs of lightweight high-strength components are common practice [13–15], For instance, within the aerospace industry, PBF holds the potential to produce lightweight and high-performance components for different systems, such as airframes, turbine blades, fasteners, casings, and engine components [16–18]. In the energy sector, PBF plays an innovative role in applications that require highly complex shapes, e.g. fuel debris filters in Boiling Water Reactor (BWR) systems for the nuclear energy industry [19], and micro-channels in proton exchange membrane fuel cell plates [20]. While, in the medical sector, PBF emerged around two decades ago with its transformative potential to produce customized implants and prostheses [21]. Despite its current capabilities, PBF poses several technical challenges, with a considerable dependency on process parameter selection, metal powder quality, and the quality and performance requirements of the final components [5, 22]. To tackle industrial challenges, PBF has seen significant advancements in recent years. Researchers have been focusing on improving multi-laser systems, scanning strategies, powder handling and recycling, metal powders, software and control systems, and sustainability and environmental impacts.

One of the significant advancements in PBF technology is the development and implementation of multi-laser systems, which can significantly increase the build rate and overall productivity by enabling simultaneous melting of powder in multiple areas. This improvement addresses the need for faster production times and higher throughput critical for large-scale manufacturing applications. Multi-laser PBF has emerged as a promising technology with the potential to enhance process efficiency and productivity [23]. Researchers have explored different approaches and innovative methods to integrate these multiple lasers. For example, Tsai et al. [24] utilized diffractive optical elements and galvanometric scanners to generate multiple laser spots from a single laser source, eliminating the need for additional laser units, and representing a cost-effective and compact approach [25]. In addition, studies have illustrated the benefits of employing multi-laser systems in PBF. Wong et al. [26] conducted trials using Inconel 625 with a multi-laser AM system, demonstrating its ability to address the challenge of low build rates, particularly in industrial settings. In addition, they found no deterioration in the mechanical and crystallographic properties of components produced through single-mode operation, underscoring the potential to enhance production rates while maintaining part quality. Moreover, multi-laser systems in PBF have created opportunities for manufacturing multi-material parts with diverse functionalities and properties. Chen [27] highlighted the capacity of PBF technology to fabricate parts with multiple functionalities, showcasing its suitability for applications in demanding environments.

Advancements in scanning strategies have also significantly contributed to the improved performance of PBF systems, enhancing the precision and quality of manufactured parts. Innovative scanning algorithms and techniques, such as optimized laser path planning and adaptive scanning, help minimize defects, reduce residual stresses, and improve mechanical properties [25]. Recent developments in scanning strategies for PBF have been pivotal in advancing additive manufacturing processes. Studies underscore the critical influence of scan strategies on the quality and characteristics of PBF-manufactured components. For instance, Masoomi et al. [23] highlighted the advantages of scan strategies with reduced track lengths aligned parallel to the part's shortest edge, resulting in enhanced outcomes. Lee and Zhang [28] indicated that rapid heating and cooling in PBF are a consequence of fast scanning speeds and low laser power. Sing and Yeong [25] emphasized the potential of specific scanning strategies for materials with low 3D printability. In addition, Batalha et al. [29] demonstrated the feasibility of designing microstructures of alloys through optimized scanning strategies. Moreover, cutting-edge strategies in multi-laser PBF processes have been introduced to improve current scanning techniques [30]. Dai et al. [31] explored the impact of scanning strategies on surface quality, highlighting the significance of contour and zigzag scanning strategies in reducing surface roughness. Shi et al. [32] found that specific strategies like the Chessboard scanning strategy can diminish heat accumulation and residual stress, resulting in well-bonded layers and flat surfaces.

In the area of powder handling, innovations in automation systems ensure consistent powder flow and distribution, crucial for maintaining the quality and repeatability of the manufacturing process. Improved powder recycling techniques have been developed to reduce material waste and lower production costs, making PBF a more sustainable manufacturing option [25]. Recent advancements in powder handling and recycling have been a significant focus in additive manufacturing research and are becoming common in PBF due to the high cost of powders [33]. Studies have indicated that the properties of the powder feedstock can change when reused, attributed to mechanisms such as

spatter generation and alterations in chemistry [34]. Recycling remains prevalent despite challenges like spatter and condensate formation [25]. Research has explored the impact of powder recycling on the mechanical properties of materials processed through PBF. Investigations have shown that after multiple recycling events, there is no significant deterioration in tensile properties, suggesting recycled powders could serve as sustainable feedstock candidates [35]. Studies have examined the effects of both recycling and rejuvenation processes on powder characteristics and part properties [36]. Moreover, significant progress has been made in monitoring and controlling the PBF process. Sensor-based monitoring has emerged as a valuable tool to address process-related issues [37]. Numerical thermal–mechanical simulations are being refined to predict defects like cracks, residual stress, and distortion [38].

Recent advancements in materials specifically designed for PBF have expanded the range of applications. High entropy alloys and high-strength aluminum alloys have emerged as key materials, offering enhanced properties [25]. New metal alloys and composite materials improve mechanical properties, enabling the production of components with superior strength, durability, and functionality for aerospace, automotive, and medical devices. Progress has been made in manufacturing soft magnetic materials like Fe–Co–V alloy, showcasing the potential for producing specialized materials [39]. Studies on materials like 17-4PH stainless steel have emphasized the importance of post-processing methods such as hot isostatic pressing (HIP) to eliminate defects [40]. In addition, magnesium alloys have shown promise for aerospace applications through PBF processing, demonstrating high relative densities and hardness exceeding those of wrought materials [41]. The shift towards multi-material additive manufacturing involves assigning different material parameters to powder particles within a single layer [42]. Innovations in lattice materials using aluminum-based alloys have been explored by varying beam diameters to control relative density [43]. Furthermore, studies on nitrogen absorption during PBF of 17-4 PH steel have enhanced our understanding of material behaviors [44]. For instance, Abedi et al. [45] investigated the high-temperature flow behavior of additively manufactured Inconel 625, emphasizing its capability to maintain exceptional strength and stability at elevated temperatures. Significant advancements have been made in the fabrication of alumina/Fe–Ni ceramic matrix particulate composites using PBF, demonstrating improved mechanical properties through innovative sintering and polymer impregnation techniques [46].

Other relevant advancements were made in software and control systems for PBF, driven by the need to enhance process reliability, repeatability, and overall quality. Researchers have focused on improving various aspects of PBF processes. Lane et al. [47] discussed using thermographic measurements to understand the PBF process and better align finite element simulations and in-situ sensing for control methodologies. Mahmoud et al. [37] highlighted the application of Machine Learning in developing in-situ monitoring systems and feedback control strategies to address challenges like poor repeatability. Pagani et al. [48] emphasized the importance of in-situ monitoring systems for detecting geometrical distortions and treating data from monitoring systems to enhance process reliability. Yadav et al. [49] also stress the significance of data treatment from in-situ monitoring systems in improving process reliability in Selective Laser Melting machines. Modaresialam et al. [50] focused on in-situ monitoring and defect detection in Selective Laser Melting processes, aiming to develop closed-loop feedback control systems for real-time quality control and process improvement in PBF. Wang et al. [51] developed model-based feedforward control systems to optimize complex geometries in Directed Energy Deposition processes, showcasing the significance of computational approaches in controlling PBF processes. Yonehara [52] emphasized the importance of quantifying surface texture and melt pool behavior for developing monitoring and feedback control systems for PBF machines.

Recent research has also highlighted the significance of sustainability and environmental impact in PBF technology. Reduction in the mass and size of mechanical parts produced through PBF is crucial for decreasing environmental impact, especially in sectors like transportation and energy [53]. Strategies in PBF manufacturing are foundational for sustainable practices, enabling the development of eco-friendly components while minimizing resource usage and environmental repercussions [54]. Energy efficiency plays a key role in enhancing resource utilization and overall green performance, emphasizing the importance of sustainable practices across various industrial sectors [55]. Integrating life cycle assessment (LCA) and linear programming tools has been suggested to improve environmental sustainability decision-making processes, showcasing the potential for more sustainable products and processes [56]. The application of green marketing principles underscores the evolving economic, social, and environmental responsibilities of businesses in addressing sustainability challenges [57]. In addition, the characterization of nanoparticle release patterns in PBF processes offers insights to enhance operational conditions and safety guidelines, contributing to the overall sustainability of additive manufacturing processes [58].

These advancements in computational control, sustainability practices, and environmental impacts highlight the continuous innovation within PBF technology. As the field progresses, it is essential to not only implement these advancements but also to quantify the pace at which technical performance improves. This leads us to consider the broader implications of innovation within additive

manufacturing. In fact, in the fast-evolving landscape of additive manufacturing, understanding, and quantizing the pace at which the technical performance of PBF increases becomes a critical factor. In high-tech sectors, it is acknowledged that innovation plays a crucial role in driving economic prosperity, with minor advancements in technology often resulting in significant competitive benefits [59–61]. The central importance of innovation underscores the need for a comprehensive grasp of the forces driving technological evolution, including accurately estimating PBF's TIR, which is crucial for various stakeholders. This understanding aids industries and businesses in strategic planning, aligns future developments with technological progress, and informs investment decisions, especially in research and development and industrial applications, targeting areas of rapid improvement. In addition, such estimation is vital not only for companies involved in the creation and production of engineering goods and services but also plays a crucial role in market forecasting for research bodies, policymakers, private and public investors, and others. It enables companies to anticipate demand shifts and adapt to evolving market dynamics, influencing technology adoption, and guiding product development to align with upcoming PBF capabilities [62–68].

To ensure that these anticipations and adaptations are beneficial, it is crucial to gauge the trajectory of technological progress and assess its congruence with the pressing demands of the industry. The concept of quantifying a technology's advancement over time was initially proposed by Moore [69] and further expanded by other authors [67, 70–76]. These studies commonly reveal an exponential relationship between performance and time, suggesting a consistent annual percentual performance increment. The Technological Improvement Rate (TIR) is a key measure for tracking the yearly performance improvement of a technological domain, indicating the annual percentage increase in its performance [72, 77, 78]. The TIR represents the improvement for a performance-related specific generic function that the technological domain is set out to achieve [77]. The performance improvement can be described by the following equation:

$$Y = Y_0 \exp(k(t - t_0)) \tag{1}$$

where Y is the performance at time t, Y_0 is the performance at a reference time, t_0, and k is the exponential constant representing the TIR. To estimate *k*, the initial step involves creating a functional performance metric (FPM) that assesses the generic function of a technological domain, incorporating factors influencing the buying choices for artifacts that utilize the technology [77]. The ideal FPM should encapsulate all potential aspects, both value-driven and cost-related, to ensure a comprehensive understanding of the technology's overall impact and appeal [79]. Prior research has analyzed a range of relevant factors in additive manufacturing technologies [72, 77–79] over time to determine their improvement rates, focusing on technical parameters like speed, accuracy, and system acquisition cost. Based on data from Wohlers' reports and additional sources it was estimated that Vat Photopolymerization technology has a yearly empirical improvement of 37.6% [79]. Subsequent research by Benson and Magee [77] demonstrated that the technological improvement rate for Vat Photopolymerization could be approximated using a collection of patents within this technological field. The estimated improvement rate from the Vat Photopolymerization patent set was 38.5%, aligning closely with the empirically derived rate of 37.6%. Subsequent patent-based studies estimated improvement rates for other additive manufacturing domains of 35.0% for inkjet-powder-based AM, 33.3% for PBF–LB/M), 16.7% for fused filament fabrication (FFF), 21.1% for nonmetal selective laser sintering (SLS), 29.4% for the whole AM technological domain [80] and 31.5% for advanced composites AM [81]. While existing literature offers profound insights into the technological improvement rates in AM technologies, there exist certain lacunae, since they mostly rely on a patent-based method.

Although an approach based on patents has gained traction and validation in the field of quantitative technology assessment, it remains an indirect metric. It is associated with an inherent degree of uncertainty, underscoring the need, when possible, for empirical studies with more direct measurements to bridge patent gaps and provide a more definitive perspective. The goal of the present study is to ascertain a robust empirical estimate for the TIR of PBF. Anchored in this purpose, our specific objectives are to define a functional performance metric for powder bed fusion and build a reliable data set of widely available technical parameters comprising the FPM. Subsequently, the TIR is estimated based on the FPM and, by applying quantitative and qualitative methods, the reliability of the FPM and estimated TIR are assessed. This study, focusing on empirically estimating how fast the performance of PBF is evolving, aims to significantly benefit industrial and academic stakeholders, guiding their investment strategies, research, and policymaking in the PBF technological domain.

This paper is structured in five sections. The data and Methods section details the methodology, including the construction of the functional performance metric and data set, and the regression analysis approach The Results and Discussion section presents the findings from the data set, including the estimated Technological Improvement Rate of PBF technology, and delves into insights derived from the results. This includes addressing data set reflections, model interpretations, limitations, material influence, and technological progress. Finally, the Conclusions wrap up the study, highlighting its significance and implications.

2 Data and methods

This section outlines the methodology utilized to collect the data, calculate the TIR of PBF, and test its reliability. Firstly, the ideal functional performance metric of PBF was defined. Through a literature review, it was identified the factors influencing the purchasing decisions for PBF technology, and it was determined which technical capability parameters comprise the FPM. These parameters must be direct quantitative measures reflecting both the value and cost of the technology to users and readily available as PBF machine specifications. Subsequently, a data-gathering process was conducted. To accurately assess the FPM's evolution over time, information was gathered relative to these PBF machine's parameters, spanning from the technology's early stages to the present. A process of data curation was conducted. This involves evaluating the reliability of data collected in terms of data source and its scarcity. Once obtained, the data in the potentially reliable data set, is fitted by a regression model, with time as the independent variable. The section concludes by detailing the quantitative and qualitative methods employed to validate the reliability of the FPM metric.

2.1 Functional performance metric construction

Being a measure of the generic function that a technological domain is trying to accomplish, the FPM includes the factors that affect the purchasing decision for the technology, these include both measures of value and measures of cost to the consumer of a technology. Gathering the data relative to the candidate parameters to form the functional performance metric used to estimate the technological improvement rates is a time-consuming process since a large amount of reliable data covering a wide timeframe is needed. Identifying suitable functional performance metrics for manufacturing technologies poses challenges given the heterogeneity of their outputs and their multiple functions that can hold different significance for various customers [82]. Past studies have defined metrics suited for different manufacturing technologies [79, 81, 83]. For manufacturing technologies, Benson [79] defined the primary attributes of interest to be speed, flexibility, quality, and cost. A knowledgeable purchaser would thus aim to optimize speed and flexibility while reducing cost and dimensional inconsistency. Consequently, a standard manufacturing metric can be depicted by the following equation:

$$\mathrm{FPM}_{\text{manufacturing technology}} = \frac{\text{Speed} \times \text{Flexibility}}{\text{Resolution} \times \text{Cost}} \tag{2}$$

Calderaro et al. [84] proposed five general competitive criteria for assessing the technological capabilities of metal AM technologies, namely, speed, flexibility, quality, cost, and sustainability. These criteria can be used to generate a generic FPM for metal AM, arranged in the following equation:

$$\mathrm{FPM}_{\text{AM Metal}} = \frac{\text{Speed} \times \text{Flexibility}}{\text{Quality} \times \text{Cost} \times \text{Sustainability}} \tag{3}$$

Equations (2) and (3) are equivalent, in the sense that the term Resolution is substituted by the general term Quality and the general term Cost of Eq. (2) is split into monetary Cost—defined just by Cost by the authors—and sustainability which represents the "cost" to the environment. Recently, Ferreira et al. [85], building on top of the work of Calderaro et al. [84], listed 20 qualitative and quantitative capability parameters to evaluate metal AM machines and classified them into one of the five competitive criteria. Table 1 presents competitive criteria for evaluating Additive Manufacturing (AM) technologies, detailing their characteristics, specific capability evaluation parameters, nomenclatures, and their quantitative or qualitative nature. A definite functional performance metric for PBF would incorporate all capability evaluation parameters representing measures of value and cost for the consumer. The capability evaluation parameters of AM Technology listed in Table 1 serve as a starting point for constructing the FPM developed in this research.

Each capability evaluation parameter is looked at to determine its legitimacy as a direct measure of value and cost. Regarding the criterion of Speed in additive manufacturing, two distinct characteristics are recognized, Manufacturing time and Total Process time. Total Process time is eliminated as a possible FPM parameter because it encompasses pre- and post-AM manufacturing accessory steps. These steps are not inherently associated with PBF technology, and their functional purpose is often related to surface quality and dimensional accuracy which are evaluated under the quality criteria. Consequently, the Machine's build rate remains the singular direct quantitative measure of value for the consumer pertinent to the Speed criterion.

The flexibility criterion splits into four distinct AM technological characteristics: geometric limitations, manufacturing dimensions, raw material, and multi-material. The technological characteristics associated with materials predominantly pertain to qualitative parameters, requiring conversion, and as such, they are not deemed integral to the FPM. Delving into the parameters within geometric limitations, they comprise wall thickness, unsupported walls, embossed/engraved details, unsupported edges, fillets, hole size, escape holes, and feature size. Notably, these parameters, while quantitative, originate from other primary parameters present in Table 1 that stand as potential candidates for FPM parameters, such as Machine

Table 1 Competitive criteria and associated capability evaluation parameters. (Adapted from Ferreira et al. 2023 [85])

Competitive criteria	Characteristic of AM technology	Capability evaluation parameters of AM technology	Nomenclature	Parameters type
Speed	Manufacturing time	Machine's build rate	Build rate	Quantitative
	Total process time	Process time of all manufacturing steps	Process time	Qualitative
Flexibility	Geometric limitations	Wall thickness	Wall thickness	Quantitative
		Unsupported walls	Unsupported walls	Quantitative
		Embossed/engraved details	Embossed/engraved details	Quantitative
		Unsupported edges	Unsupported edges	Quantitative
		Fillets	Fillets	Quantitative
		Hole size	Hole size	Quantitative
		Escape holes	Escape holes	Quantitative
		Feature size	Feature size	Quantitative
	Manufacturing dimensions	Machine's build volume	Build volume	Quantitative
	Raw material	Metal alloys	Raw material	Qualitative
	Multi-material	Multi-material feature	Multi-material	Qualitative
Quality	Surface quality	Surface finish (Ra)	Surface finish	Quantitative
		Layer thickness	Layer thickness	Quantitative
	Precision	Machine's dimensional accuracy	Minimum dimensional accuracy	Quantitative
		Machine's dimensional detail	Minimum detail resolution	Quantitative
	Mechanical properties	Component's density	Density	Quantitative
Cost	Manufacturing cost	Energy consumption	Energy consumption cost	Quantitative
		Machine's acquisition cost	Acquisition cost	Quantitative
Sustainability	Environmental impact (EI)	EI raw material	Environmental impact	Quantitative
		EI energy consumed in printing		Quantitative

dimensional accuracy, resolution, and layer thickness. To avoid metric redundancy, parameters connected to Geometric limitations are ruled out. The final parameter under Flexibility is the Machine's build volume, which serves as a direct consumer value measure and is thus shortlisted for inclusion in the FPM.

In the third competitive criterion, quality, the capability parameters encompass surface finish, layer thickness, machine's dimensional accuracy, machine's dimensional resolution, and the component's density. All parameters are straightforwardly seen as relevant values and costs for consumers and thus must be considered in the FPM. The technology capability parameters under the Cost criterion relate to costs arising from the Machine's energy consumption and the Machine's initial purchase cost. Both are unequivocal direct measures of cost for the consumer and are, therefore, relevant for the FPM.

Finally the technology capability parameters about sustainability address the environmental ramifications linked with the raw material utilized in PBF, the environmental Impact (EI) of raw material, and the EI of energy consumption during production. These are salient measures of environmental cost that strengthen the comprehensive nature of the PBF's FPM. The parameters representing cost and value for the consumer can then be substituted by their constituent variables. The resultant FPM for PBF can be described by the following equation:

$$\mathrm{FPM}_{\text{AM Metal}} = \frac{\mathrm{SBR} \times \mathrm{FBV}}{\mathrm{QSF} \times \mathrm{QLT} \times \mathrm{QA} \times \mathrm{QR} \times \mathrm{CEC} \times \mathrm{CA} \times \mathrm{EIRM} \times \mathrm{EIEC}} \quad (4)$$

Speed: build rate (S_{BR})
Flexibility: build volume (F_{BV})
Quality: surface finish (Q_{SF})
Layer thickness (Q_{LT})
Accuracy (Q_A)
Resolution (Q_R)
Cost: energy consumption (C_{EC})
Acquisition (C_A)
Sustainability: environmental impact of raw material (EI_{RM})
Environmental impact of energy consumption (EI_{EC})

2.2 Data set construction

2.2.1 Data sources and collection method

Several sources of information containing data relative to the parameter's constituents of the above-derived FPM were consulted. The first data source considered is the records of technology-producing firms. Although large firms may have comprehensive archives from which historical data from performance-related parameters are available, data extraction is not always straightforward, and some data remain confidential for competitive reasons [79]. Another source of data provided by technology-producing firms is Product Specifications/datasheets. These are company documents detailing their product's capabilities. While highly informative, their primary function is disclosing product capabilities for marketing purposes which in some industries potentially affects the accuracy of the disclosed data [79]. Trade Magazines are another available source of data. They offer continuous updates on technological progress but have a commercial orientation and thus potentially suffer from the same downside of product datasheets. Scientific Literature, another relevant data source, is a peer-reviewed medium with data sometimes sourced from the above. It has the advantage of providing a neutral perspective from various producers. Another data source considered, Industry Reports, paints a full industry picture. Private versions are detailed but may lack references and be costly, while public versions give a wider view that may not always represent peak yearly performance. Lastly, patents, issued by governmental bodies, grant inventors rights to their creations and detail the technology involved. These descriptions often cover performance parameters and methodologies. Although patents provide insights into technological capabilities, their primary focus is on novelty rather than comparative metrics. Extracting data from patents can be challenging due to technical and legal language, but they remain vital for understanding industry trends and competition [79].

Figure 1 illustrates the data collection and curation steps followed to construct the data set. Our data collection process was methodical and focused on completeness. First, we constructed a list of all commercially available PBF machines to cover the full spectrum of available technology by scraping catalogs of manufacturers, commercially available machine data sets, and publications of the trade. Next, we collected relevant documentation for each machine from the abovementioned sources, including product datasheets, trade magazines, scientific publications, and industry reports. This documentation provided detailed information on the machines' parameters. By systematically extracting data from these diverse sources, the data set was populated.

2.2.2 Data curation

After systematically populating the data set with all available information related to the machine parameters, we conducted a thorough assessment of each parameter (Step 3 of Fig. 1). Our goal was to construct the most reliable functional performance metric (FPM). To achieve this, we required data that was significantly large in quantity, reliable, and spanned the decades of the technology's existence. The curation process involved evaluating the completeness and consistency of the data for each parameter to ensure the reliability and validity of our analysis. The data availability and data heterogeneity were the two main criteria used for parameter inclusion/exclusion. For a certain machine parameter, if the available data were limited to the point that including it would result in an FPM with too few data points, thus compromising its reliability, the parameter was excluded from the data set and was not used in the construction of the FPM. For certain parameters, manufacturers provide varying types of data, and consolidating these disparate data types into a single parameter is challenging, serving also as a criterion for parameter exclusion. In our efforts to ensure the reliability of the FPM, we employed the following measures:

- Collected data that systematically showed a lack of uniform conditions was discarded. Examples of this were precision and accuracy-related data as they lacked a uniform metric.
- Data sources that showed systematic incongruencies with other sources deemed more reliable (e.g., websites vs.

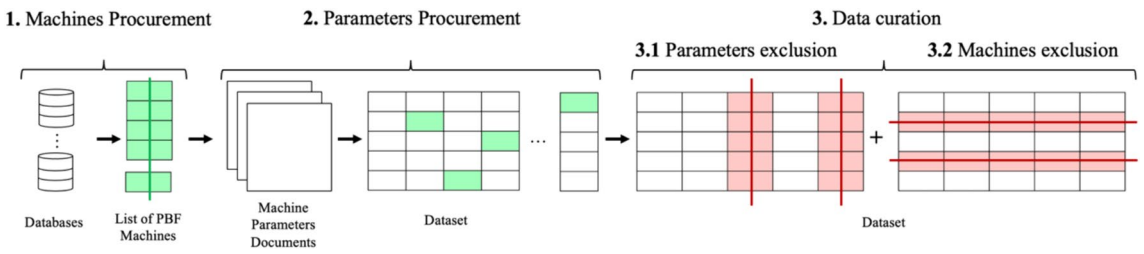

Fig. 1 Data collection and curation process

published trade reports) were not considered. This led to the exclusion of several sources of cost data, resulting in very few cost data points being incorporated into the data set. Consequently, the cost parameter was discarded.
- Reported data related to the parameters build rate, build volume, and layer thickness did not show any evidence of a lack of repeatability. The collected data related to these parameters were only obtained from direct sources, i.e., machine manufacturers' datasheets.

After the parameter curation process, we further refined the data set by discarding any machines that had missing data for the considered parameters. Through an exhaustive process of data collection, data source assessment, and comparison, we are convinced that the data used to construct the FPM is highly reliable.

2.3 Regression analysis

The rate of technological improvement for PBF technology is estimated through the application of a linear regression model on the logarithmically transformed data constructed using the FPM. This logarithmic transformation serves a dual purpose: it normalizes the distribution of performance metrics and linearizes the exponential growth curve characteristic of technological advancements. The transformation is crucial as it ensures a constant variance of the performance metric—a necessary condition for the applicability of linear regression [86]. The performance metric for individual PBF machines is computed using a modified version of Eq. (4), introduced in the results and discussion section. For regression analysis purposes, we reformulate the model from its initial exponential expression $Y = Y_0 \exp(k(t - t_0))$ (1) into a log-linear format by taking the natural logarithm of the performance values:

$$\log(Y) = \log\left(Y_0\right) + k\left(t - t_0\right) \tag{5}$$

here Y represents the original performance metric, t is the temporal variable, Y_0 denotes the baseline performance, and t_0 is the reference time for the baseline performance. We then express the log-transformed model as

$$\log(Y) = \beta_0 + \beta_1 t + \epsilon \tag{6}$$

where $\log(Y)$ is the natural logarithm of the FPM, β_0 is the y-intercept on the log scale, and β_1, the slope of the regression line upon the log-transformed data, provides an estimation of the improvement rate k. When we exponentiate the log-linear model to return to the original performance metric scale, the term e^{β_1} k, the compound annual performance improvement rate of the technology. To clarify, the linear regression model presupposes that the errors ϵ in the predictions are independently and identically distributed (i.i.d.) with a mean of zero. This assumption is corroborated through a detailed residual analysis, which examines the residuals for patterns that might indicate violations of i.i.d. conditions, such as non-randomness or heteroscedasticity.

There are two main ways of estimating the improvement rate, k: either using all the points in the data set for the regression, or as is most common, and the strategy used in this research, only considering the non-dominated data points. These non-dominated points are essentially record-breaking machines with the highest performance up to the date of their release [79]. This choice is justified by focusing on capturing the leading edge of performance improvements, i.e., the technological state-of-the-art, over time.

2.4 Reliability evaluation of the functional performance metric

The reliability of the constructed FPM is crucial to validate the accuracy and applicability of the estimated TIR. Accordingly, we employed an array of quantitative techniques to evaluate the FPM's reliability. These approaches include methods for statistical significance testing alongside model fit assessments to ensure the observed relationships are substantiated and not simply due to stochastic variance. Together, these metrics give us a detailed view of the FPM's reliability, reinforcing the credibility of TIR findings and their relevance to the ongoing development of PBF. The model's limitations are acknowledged, such as the scope of the data set, which is constrained by the availability of PBF commercial machine data. Despite these constraints, the estimated k offers a significant insight into the rate of improvement of PBF technology's performance over time, providing a valuable indicator for stakeholders in the field.

2.4.1 Confidence and prediction intervals for linear regression

The confidence interval (CI) for the regression line is a range within which we can expect the true regression line to lie with a specified probability (usually 95%). It accounts for the variability in the data and the uncertainty in estimating the model parameters. It estimates where the mean response (the expected value of Y) for a given X lies, not the individual future observations. The CI for the predicted values at a specific t_0 value is given by

$$\left|\hat{\mu}_{y|t_0} - \mu_{y|t_0}\right| \leq T_{n-2}^{0.975}\hat{\sigma}\sqrt{\frac{1}{n} + \frac{(t_0 - \bar{t})^2}{\sum_{i=1}^{n}(t_i - \bar{t})^2}} \tag{7}$$

where $\left|\hat{\mu}_{y|t_0} - \mu_{y|t_0}\right|$ is the absolute difference between the estimated and the true population means, $T_{n-2}^{0.975}$ is the critical

value from the t-distribution for a 95% confidence level and $n-2$ degrees of freedom. $\hat{\sigma}$, is the standard error of the regression, t is a specific value of the independent variable, and $\bar{t}$ is the mean of the independent variable. The standard error of the regression is a measure of the standard deviation of the residuals, i.e., the scatter of the observed values around the regression line, and is given by

$$\hat{\sigma} = \sqrt{\frac{\sum_{i=1}^{n}(y_i - \hat{y}_i)^2}{n-2}} \tag{8}$$

where y_i is the observed value of the dependent variable for the ith observation. $\hat{y}_i$ is the predicted value of the dependent variable for the ith observation, given by the regression model and $\sum_{i=1}^{n}(y_i - \hat{y}_i)^2$ is the sum of the squared residuals, representing the sum of the squared differences between each observed value and its predicted value. The standard error of the regression provides an estimate of the precision of the regression model. A smaller standard error indicates that the model's predictions are more precise, meaning they're closer to the actual data points. The prediction interval (PI) gives a range within which we expect future individual observations to lie, with a certain level of confidence. It accounts for the variability around the individual predicted value of Y, which includes both the error in estimating the true regression line (as with the CI) and the variability of the individual observations around the regression line. Because the PI accounts for more sources of variability, it is wider than the confidence interval, reflecting greater uncertainty about where any single observation will fall. The PI for the predicted values at a specific t_0 value is given by

$$\left|\hat{\mu}_{y|t_0} - \mu_{y|t_0}\right| \leq T_{n-2}^{0.975}\hat{\sigma}\sqrt{1 + \frac{1}{n} + \frac{(t_0 - \bar{t})^2}{\sum_{i=1}^{n}(t_i - \bar{t})^2}} \tag{9}$$

The unit value, *1*, is the first component inside the square root and accounts for the variability of an individual observation around the mean response. The second component, $\frac{1}{n}$, adjusts for the precision of the estimate of the mean response at t_0. The third component, $\frac{(t_0-\bar{t})^2}{\sum_{i=1}^{n}(t_i-\bar{t})^2}$, adjusts for the leverage of t_0—the distance of t_0 from the mean of t relative to the spread of all t values, which affects the precision of the prediction. Overall, the PI provides a range that is expected to contain the actual observation for a given time value t_0 with a specified confidence level. It's wider than the CI for the mean response because it incorporates the additional variability of individual observations.

2.4.2 Goodness of fit

Evaluating the residuals and the overall goodness of fit is an essential step in validating the assumptions of linear regression and the model's predictive power.

Coefficient of determination (R^2): The R^2 value is a measure that represents the proportion of the variance for the dependent variable that's explained by the independent variables in the model. It is given by the formula:

$$R^2 = 1 - \frac{\text{RSS}}{\text{TSS}} \tag{10}$$

where RSS is the variation explained by the model given by the residual sum of squares and, TSS is the total variation in the model given by the total sum of squares. The closer the value is to 1, the better the model explains the variability of the response data around its mean.

Chi-squared (χ^2): The Chi-squared test is a measure of how expectations compare to actual observed data. In the context of regression analysis, it is used to assess the deviation of the observed values from the expected values under the model. The equation for Chi-squared is

$$\chi^2 = \sum_{i=1}^{n}\frac{(y_i - \hat{y}_i)^2}{y_i} \tag{11}$$

where y_i is the observed value, and $\hat{y}_i$ is the expected (or predicted) value according to the model. The summation runs over all data points.

Reduced Chi-squared (χ^2_{red}): The Reduced Chi-squared statistic adjusts the Chi-squared value for the number of degrees of freedom in the model. It provides a more normalized measure of goodness of fit. The reduced Chi-squared is calculated as

$$\chi^2_{\text{red}} = \frac{\chi^2}{\text{dof}} \tag{12}$$

where dof represents the degrees of freedom, typically calculated as the number of observations minus the number of parameters in the model.

F test: The F test is conducted to test the overall significance of the regression model. The null hypothesis is that all regression coefficients are equal to zero. The F-statistic is calculated by

$$F = \frac{(\text{TSS} - \text{RSS})/p}{\text{RSS}/(n-p-1)} \tag{13}$$

where TSS is the total sum of squares, RSS is the residual sum of squares, and p is the number of parameters in the model and n is the number of observations. A significant F test indicates that the observed R^2 is reliable and not a result of the number of predictors.

T test for regression coefficients: In linear regression analysis, the T test is utilized to ascertain the statistical significance of individual regression coefficients. This test determines whether the estimated coefficient for a predictor variable is statistically different from zero, indicating that the predictor has a meaningful impact on the dependent variable. For a given regression coefficient β_j, the t value is calculated using the following formula:

$$t = \frac{\widehat{\beta j}}{\mathrm{SE}(\widehat{\beta j})} \tag{14}$$

Here, $\widehat{\beta j}$, is the estimated coefficient for predictor variable j and $\mathrm{SE}(\widehat{\beta j})$ denotes the standard error of the estimate for βj. The standard error is a measure of the precision of the estimate, reflecting the variability of $\widehat{\beta j}$ across different samples. The computed t value is then compared to the critical value from the t-distribution corresponding to the chosen significance level α typically 0.05, with $n-p-1$ degrees of freedom, where n is the total number of observations and p is the number of predictors (excluding the intercept). The critical t value can be represented as $t_{\mathrm{critical}} = t_{\alpha/2,n-p-1}$. If the absolute value of the computed t value for β_j is greater than critical t_{critical}, we reject the null hypothesis that $\beta_j = 0$, thereby affirming the significance of the predictor in the model. Conducting a T test for each coefficient elucidates the unique contribution of each predictor variable to the linear regression model, identifying the variables that are most influential in predicting the outcome variable. Combined with goodness-of-fit measures such as R^2 and the F test, the T test helps in verifying the reliability and validity of the regression model.

2.4.3 Point removal method

Our reliability evaluation is extended by applying the Point Removal Method (PRM), which assesses the TIR's robustness by selectively omitting and reintegrating data points. PRM was designed to examine the consequences of missing data within a technological improvement curve and manage scenarios with sparse data points [79]. The steps of the PRM algorithm are illustrated in Fig. 2. Initially, a specific data point i is removed. Following its exclusion, the k and R^2 values are recalculated. This process is repeated iteratively for all data points of the FPM data set. After cycling through all points, a summary of all k and R^2 values is compiled. Finally, analysis to evaluate their mean and variance.

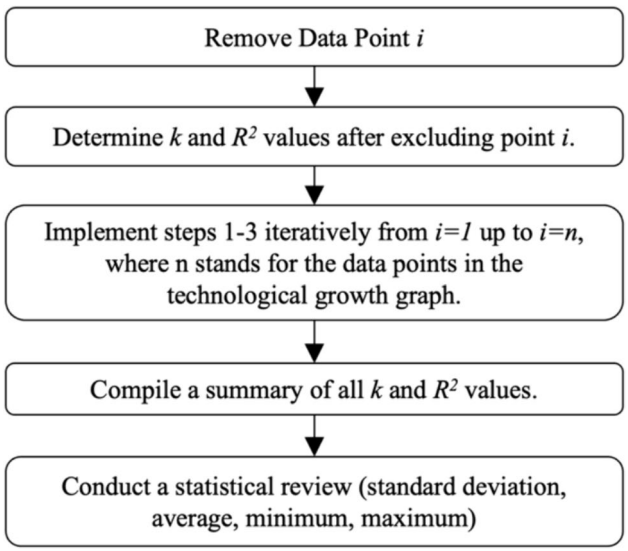

Fig. 2 Sequential steps of the point removal method

3 Results and discussion

3.1 Resultant data set

The data set building process started with gathering information on PBF machines that have been commercially available throughout the lifetime of the technology. We identified over 250 PBF machine models. The next step involved collecting documents from various sources related to these machines to extract machine parameter data, thereby populating the data set.

In the data curation phase, the first step was to exclude machines for which no information about the release date was available, as performance must be assessed over time. We then assessed how each parameter contributed to the sparsity of the data set, identifying which parameters would reduce the reliability of the FPM if included. Through an analysis of missing values, sparsity, and determination of usable parameters, we found that the two parameters related to the sustainability, the environmental impact of raw material and the environmental impact of energy consumption, the cost-related parameter, energy consumption, and quality-related parameter surface finish had almost no data collected (< 10 datapoints each) and thus could not be considered for the FPM. Although we collected slightly more data for the quality-related parameters, accuracy and resolution, these were also excluded due to inconsistencies in the data reported by different manufacturers. Some manufacturers reported XY accuracy, some overall accuracy, and others were unclear about what they were referring to, making it hard to standardize these parameters. The acquisition cost was also neglected as a parameter for the FPM. An insufficient number of data points was collected (< 30), and the

sources were considered unreliable since they were often not direct sources (machine manufacturers) and multiple sources frequently reported different prices for the same machines, further reducing the reliability of the cost data.

As a result of this curation process, from the ten parameters initially defined in Eq. (4), three—build rate, build volume, and layer thickness—were deemed suitable for inclusion in the data set used to estimate the performance improvement rate. A more in-depth assessment of the seven excluded parameters due to lack of data availability and data heterogeneity is conducted in the next subsections. The resultant practical FPM used to assess the performance improvement rate of PBF is given by the following equation:

$$\mathrm{FPM}_{\mathrm{PBF}} = \frac{\mathrm{SBR} \times \mathrm{FBV}}{\mathrm{QLT}} \tag{15}$$

The data set comprises 121 technological performance observations of 48 PBF machines made commercially available between 1995 and 2022. In the data set, every observation represents a unique instance of the technological performance construct as defined by the FPM. This includes a specific combination of build volume, build rate, and layer thickness for a given PBF machine, characterized under a particular material and configuration settings. In this context, it's worth noticing that some machines have contributed multiple data points to the data set. For a given machine, while the build volume remains constant across various observations, variations are observed in both build rate and layer thickness. These variations are due to differences in machine settings and the use of various metal alloys in the manufacturing process. The alloys used include copper, nickel, aluminum, steel, and titanium, in addition to instances where the material was unspecified.

3.1.1 Parameter data included in the data set

Build volume, typically measured in dm^3, is the maximum three-dimensional space within which a machine can fabricate an object. It's a key consumer parameter widely available in manufacturers' datasheets, making it a robust candidate for inclusion in the FPM. The build rate, measured in cm^3/hr, indicates the speed of part production. This parameter, also often present on datasheets, varies depending on, several other parameters such as material and layer thickness. However, manufacturers sometimes omit the material types and layer thickness associated with the disclosed build rate, leading to potential overestimation of capabilities. To address this, we only considered build rates in our data set when they were explicitly paired with the layer thickness at which they were achieved, ensuring a strict pairing of build rate and layer thickness. Layer thickness refers to the height of each successive layer of material that's fused during manufacturing. It's interdependent on factors like print speed, energy input, and material properties; its adjustment can thus directly affect resolution and part properties. Manufacturers frequently disclose this parameter in machine datasheets, either as the lowest achievable thickness or as a range. In addition, metal powder datasheets occasionally showcase it in tandem with the related build rate.

3.1.2 Parameter data excluded from the data set

The exclusion of certain parameters due to data sparsity and inconsistency was a critical aspect of our data curation process. Surface finish, which indicates the surface quality of printed components, is influenced by several parameters such as layer thickness and material attributes. Despite its relevance, its limited inclusion in data sources did not meet the criterion for data availability. Similarly, accuracy, the degree to which the printed object matches the original designed specifications, and resolution, defining the minimum feature size the machine can produce, were also excluded from the data set due to limited and inconsistent data. Manufacturers reported these parameters variably, with some specifying XY accuracy, some overall accuracy, and others providing unclear metrics, leading to potential discrepancies. Establishing a uniform standard for reporting these parameters would significantly enhance the robustness of future data sets.

Energy consumption, while relevant, was excluded due to its complex nature and the variability in how it is reported. Manufacturers provide several energy-related parameters, such as power supply specifications and maximum or typical power consumption. However, these metrics do not fully capture the dynamic nature of energy use during actual operation. PBF printing is a multi-step process where energy consumption is influenced by various dynamic factors, and simple static measurements are unlikely to accurately reflect the machine's energy efficiency under real-world conditions. Comprehensive energy consumption data is crucial for assessing the sustainability of PBF machines but requires a more detailed approach beyond the scope of this study.

Machine acquisition costs were also excluded due to the lack of reliable data. These costs are not systematically provided by manufacturers and, when available from sources such as industry publications, trade magazines, and websites, often exhibit significant discrepancies for the same machines. The inclusion of such inconsistent and unreliable data could introduce significant biases into the FPM. In addition, acquisition costs are influenced by numerous external factors, such as market conditions, geographic location, and purchasing agreements, which are not directly related to the technological performance or capabilities of PBF machines. Therefore, focusing on build rate, build volume, and layer

thickness provided a more objective measure of machine capabilities.

The sustainability criterion primarily assesses the environmental impact of the PBF manufacturing process, considering both raw material usage and energy consumption during machine operation. However, while these are crucial elements in developing any technological performance metric, comprehensively evaluating such impacts and costs remains a complex challenge. The FPM presented in this study does not include both sustainability parameters: the environmental impact of raw material and environmental impact of energy consumption, due to insufficient data. Future efforts could benefit from more standardized reporting practices to ensure these crucial environmental aspects are better represented.

By excluding less reliable parameters and focusing on build rate, build volume, and layer thickness, the data set construction process reflects the technological progress of PBF machines over the years. These metrics provide a more direct and objective measure of the machine's capabilities, ensuring the FPM is robust and accurately reflects the performance of PBF machines. Standardizing the reporting of key parameters and incorporating more detailed environmental impact data and quality-related metrics would significantly enhance the quality of future data sets and provide a more comprehensive understanding of PBF technology's capabilities and improvements.

3.2 Reflections on the data set

The resultant data set encompasses 121 observations from 48 PBF machines commercially available between 1995 and 2022. This period captures all phases of PBF technology's growth, reflecting the industry's maturation and innovation. Notably, some machines contribute multiple data points due to varying machine settings and material use. The variation in build rates and layer thicknesses, in particular, is indicative of the nuanced capabilities of these machines when adjusted for different metals and operational conditions. The inclusion of diverse alloys such as copper, nickel, aluminum, steel, and titanium further improve the data set's richness, allowing for a multifaceted view of how material choice influences PBF machine parameters.

The data set's construction reflects the technological progress of PBF machines over the years. By including parameters that are consistently reported and directly related to the machine's performance, the data set provides a reliable basis for estimating the TIR of PBF technology. The exclusion of less reliable parameters ensures that the FPM is robust and accurately reflects the capabilities of PBF machines. The findings from this data set highlight the need for improved data collection and reporting practices in the additive manufacturing industry. Standardizing the reporting of key parameters would enhance the quality of future data sets and provide a more comprehensive understanding of PBF technology's capabilities and improvements. In addition, incorporating more detailed environmental impact data and quality-related metrics would offer a fuller picture of PBF's performance and sustainability.

3.3 Distribution and temporal evolution of machine parameters

In this subsection, we briefly present the distribution and temporal evolution of the collected data relative to machine parameters used to construct the PBF performance metric. The objective is to elucidate how the characteristics of PBF machines have progressed over time, revealing trends and patterns in their development. Figure 3 shows the log of the build volume of PBF machines as a function of their release date, offering insights into the machines' increasing capacity to produce larger parts over time. The regression fit, $Y = -3.27 \times 10^2 e^{0.165t}$, with an R^2 value of 0.924, indicates a strong correlation between time and build volume for the record-breaking machines. The non-dominated empirical data points—those representing the most efficient machines in terms of build volume—are highlighted in blue. These points, alongside the regression line, indicate a clear trend of growth in build volume—16.5% a year—underscoring the technological progress within the field. Figure 4 demonstrates the distribution of build volumes across all machines included in the study. The boxplot provides a visual summary of the data set's central tendency and dispersion, with outliers denoted by '×' markers indicating machines that significantly deviate from the rest. The bulk of the data congregates at lower build volumes, indicating a common standard for PBF machines, while the outliers suggest a minority of machines possess substantially higher build capacities.

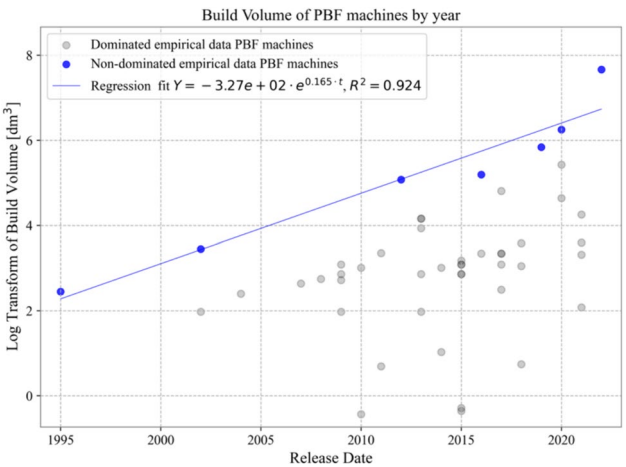

Fig. 3 Build volume over time

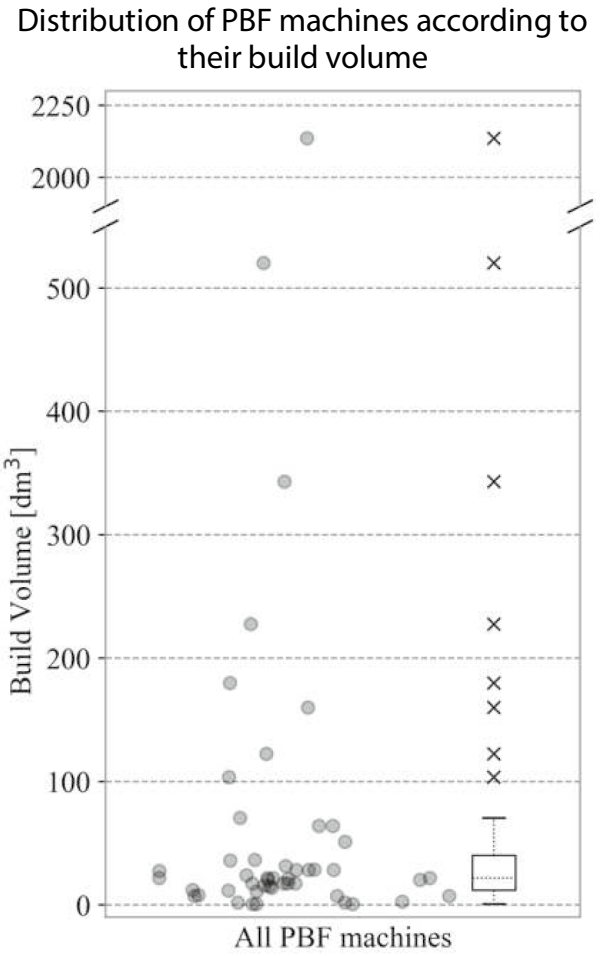

Fig. 4 Build volume distribution

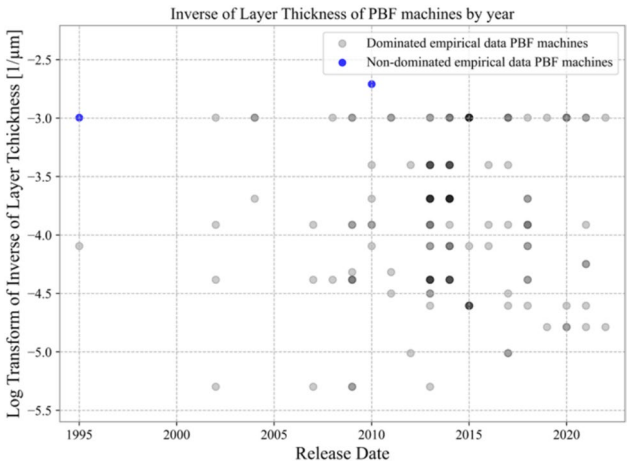

Fig. 5 Layer thickness over time

The graphs not only chart an upward trajectory in build volume over time but also capture the technological diversity within PBF machinery, showing a range of build volumes that underscore the industry's advancement towards larger-scale production capacity. This temporal evolution is marked by both a common standard in build volume across many machines and outliers, which reveal a push for increased build capabilities in the latest machine generations.

Figure 5 displays the trend in the inverse of layer thickness of PBF machines over time. Non-dominated data points are indicative of machines with the capability of producing components with the smallest layer thicknesses. The data suggest that no trend of increasing or decreasing layer thickness can be observed. The commercially available machines throughout the timeline of Fig. 5 are capable of manufacturing components using layer thicknesses roughly between 20 and 200 µm. Figure 6 shows the variability in layer thickness for machines categorized by the type of metal alloy used. Each boxplot corresponds to a different alloy category, revealing the median layer thickness, the interquartile range, and any outliers within each group. The data suggest no significant differences between the alloys, as copper, nickel, aluminum, steel, and titanium exhibit similar variability in layer thickness. The 'Not specified' category, which contains data points relative to maximum and minimum layer thicknesses for which the metal alloy was not specified by the manufacturer, contains the widest range of thicknesses, reflecting a diverse set of machine working setups.

Figure 7 provides a visual representation of the build rate of PBF machines through the years, depicted by a regression line with the equation $Y = -2.96 \times 10^2 e^{0.015t}$ and an R^2 value of 0.909. The graph highlights non-dominated empirical data points in blue. The trendline shows a clear increase in build rate capabilities over time, suggesting continuous improvements in PBF technology. This upward trend points to the industry's efforts to enhance the efficiency and productivity of PBF machines, reflecting advancements in machine design and operational parameters. The scatter of data points also underscores the variability in performance among different machines, with newer models tending to offer higher build rates, in line with technological progress. Figure 8 provides a look at the build rates of machines in relation to the metals they process. The boxplots, color-coded by alloy type, display the range of build rates for copper, nickel, aluminum, steel, titanium, and unspecified alloys. Each boxplot represents the central tendency and dispersion of the build rates within each category, with outliers marked to highlight exceptional cases. The build rates of PBF machines vary significantly depending on the type of metal alloy used. For instance, cobalt alloys exhibit build rates ranging from 6.12 to 55.44 cm^3/h, reflecting a moderate build rate spectrum. Nickel alloys, on the other hand, show a wider range of build rates, from 12.96 to 132.48 cm^3/h, suggesting more versatility and higher maximum build

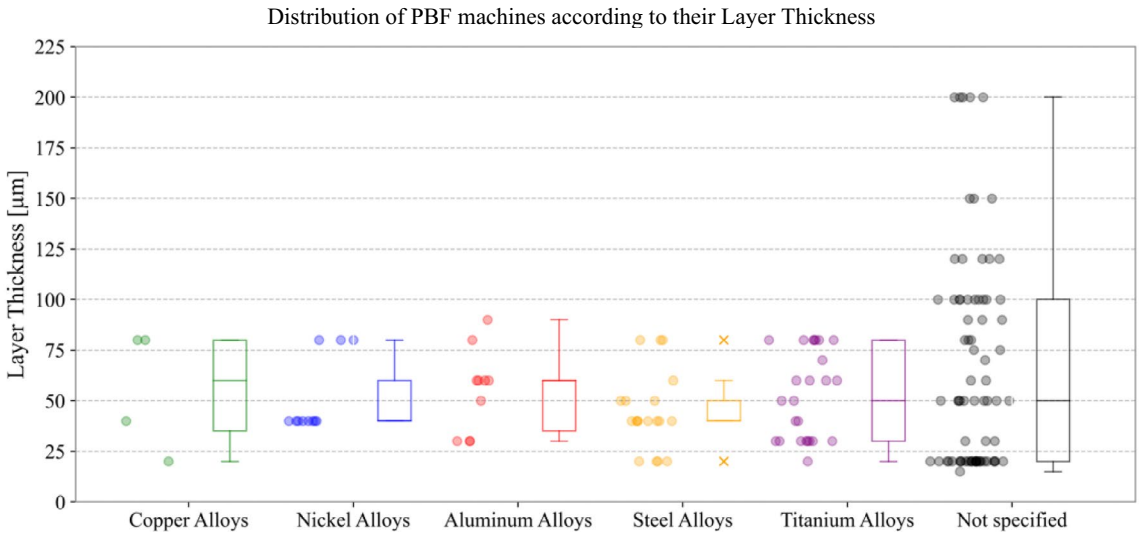

Fig. 6 Distribution of layer thickness

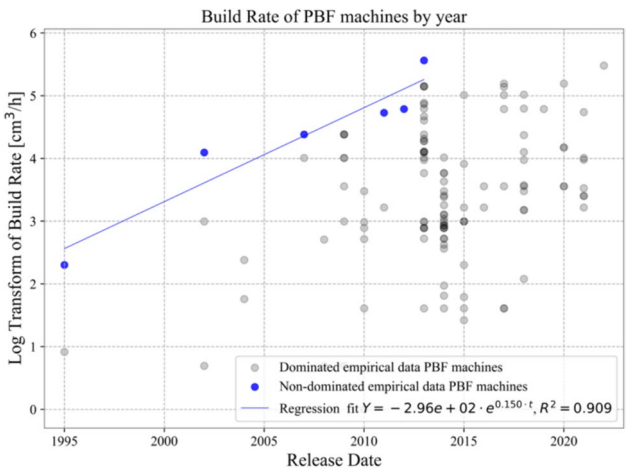

Fig. 7 Build rate over time

rates. Aluminum alloys demonstrate even higher build rates, with values ranging from 18.72 to 260.64 cm^3/h. This highlights aluminum's suitability for applications requiring rapid manufacturing speeds. Similarly, titanium alloys also show a broad range of build rates from 6 to 180.0 cm^3/h, indicating their adaptability to various manufacturing needs while maintaining high strength-to-weight ratios. Steel alloys present a diverse build rate spectrum, from 2.5 to 120.96 cm^3/h, showcasing the material's flexibility in balancing build speed and part quality. The varied build rates across these different metal alloys illustrate the importance of material selection in optimizing the build rate and overall productivity of PBF machines.

3.4 Estimated technological improvement rate

To estimate the technological improvement rate (TIR) of PBF technology, we conducted a linear regression analysis using the functional performance metric (FPM) defined by the following equation:

$$\mathrm{FPM} = \frac{\mathrm{SBR} \times \mathrm{FBV}}{\mathrm{QLT}} \left[cm^4/h\right] \tag{16}$$

where SBR is the speed parameter build rate measured in cubic centimeters per hour (cm^3/h), FBV is the flexibility parameter build volume measured in cubic decimeters (dm^3) and QLT is the quality parameter layer thickness measured in micrometers (µm). After we performed a statistical analysis of the linear regression model focused on key metrics including the Confidence Interval (CI) and Prediction Interval (PI). Figure 9 illustrates the performance of PBF machines over time, as determined by linear regression analysis on log-transformed data. The graph highlights non-dominated empirical data points in blue, representing the performance of record-breaking PBF machines, against the remainder of dominated data in grey, indicating the performance of the remainder of PBF machines. The regression, defined by the equation $Y = -5.26 \times 10^2 + e^{0.268t}$, was performed with 11 observations—data points relative to the performance of record-breaking machines. The slope of the regression line was determined to be 0.268, i.e. Powder Bed Fusion technology was estimated to be improving in performance at a yearly rate of 26.8%. Regression has an R^2 value of 0.911, indicating that the model explains a significant portion of the variance in the dependent variable. This high R^2 value points to the predictive ability and reliability of the model. The

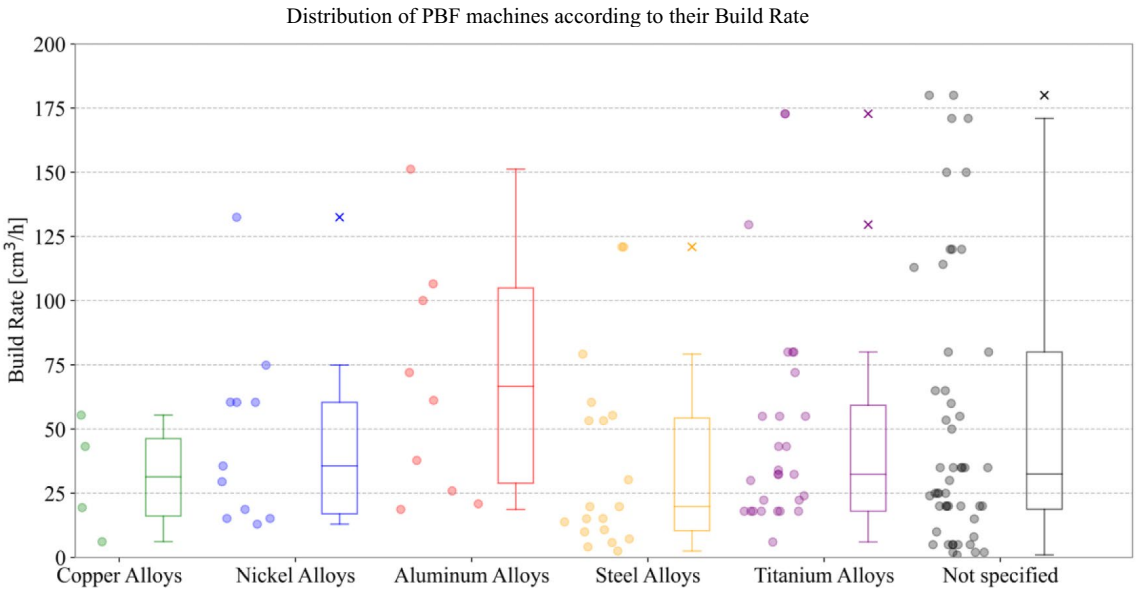

Fig. 8 Distribution of build rate

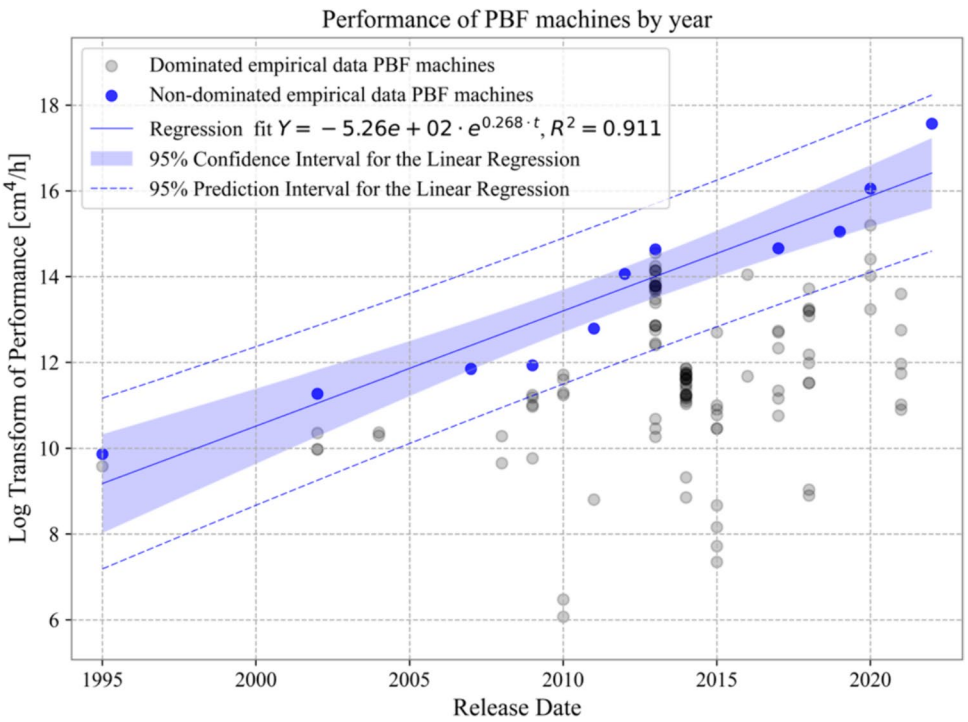

Fig. 9 Estimated performance improvement rate according to the defined functional performance metric calculated for the collected non-dominated machine data points

solid blue line represents this regression fit, with the shaded area around it, indicating the 95% confidence interval, showcasing the range within which we expect the true regression line to fall. In addition, the dashed lines delineate the 95% prediction interval, predicting the range of future observations with a given level of confidence. This visualization not only confirms the improving trend in PBF machine performance but also quantifies the inherent uncertainty in the data and the model predictions.

A summary of the regression and statistical variables is given in Table 2. The calculation of the 95% confidence interval for the slope shows that PBF is most likely improving not slower than 20.5% and improving not faster than 33.1% a year. The Chi-squared (χ^2) value of 0.026 indicates a low level of error in the model's predictions. This was

Table 2 Statistical variables of the regression

Parameter	Value
Number of observations (n)	11
Number of parameters (m)	2
Degrees of freedom (dof)	9
Slope (k)	0.268
R-squared (R^2)	0.911
95% confidence interval for slope	[0.205, 0.331]
t-statistic (t)	2.26
Chi-squared (χ^2)	0.026
Reduced Chi-squared (χ^2_{red})	0.0029
Standard deviation of the error (S_{err})	0.718
T-statistic for slope	− 9.35
p value for slope	1.00E− 05
F-statistic	10.11
p value for F test	0.01

supported by the reduced Chi-squared (χ^2_{red}) value of 0.0029, which suggested a good fit for the model. The standard deviation of the error, measuring the variation in the model's predictions, was calculated at 0.718. The t-statistic of 2.26 is important for calculating confidence and prediction intervals, signaling a departure from the null hypothesis that's clear but not extreme. It's enough to influence our confidence and prediction intervals, yet it doesn't point to an exceptionally large effect. Therefore, the t-statistic of 2.26 guides how we understand our model's accuracy without suggesting a drastic difference from expected values. The T test for the slope showed a t-statistic of − 9.35 with a p value of 1e− 05, confirming the statistical significance of the slope. The F test for overall model significance yielded an F-statistic of 10.11 and a p value of 0.01, verifying the model's robustness and reliability. These statistical measures, including CI and PI, demonstrate the model's capability to accurately predict the dependent variable, underlining its statistical significance and practical use.

Figure 10 presents a dual analysis of the estimated slope (k)–rate of improvement in powder bed fusion technology performance. The left panel shows the probability density function (PDF), mapping the likelihood of different slope values within the 95% confidence interval. The right panel displays the cumulative density function (CDF). Together, these plots quantify the statistical certainty of the slope estimate, providing a nuanced understanding of the rate at which this technology is advancing.

The results from the application of the point removal method (PRM), shown in Table 3, provided valuable insights into the robustness and empirical effects of missing data points on the technological improvement curve. This method, aimed at complementing traditional statistical analyses, proved to be important in understanding the robustness of the TIR. PRM results show a mean k value of 0.269, with a standard deviation of 0.013. This indicates a moderate spread around the mean, suggesting that the TIRs are reasonably consistent across different subsets of the data. The minimum and maximum k values were 0.243 and 0.303, respectively, providing a range within which the majority of the TIR values lie. For the R^2 values, the mean was calculated at 0.912, accompanied by a standard deviation of 0.009. This high mean value of R^2 highlights the model's strong explanatory power, even with the removal of individual data points. The minimum R^2 value was 0.899 and the maximum was 0.928, further emphasizing the model's stability and robustness across various data subsets. These results from the PRM demonstrate not only the resilience of the estimated k to variations in data but also underscore the reliability of our model in capturing the technological

Table 3 Statistics of k and R^2 values resulting from the point removal method

	k	R^2
Mean	0.269	0.912
Std	0.013	0.009
Min	0.243	0.899
Max	0.303	0.928

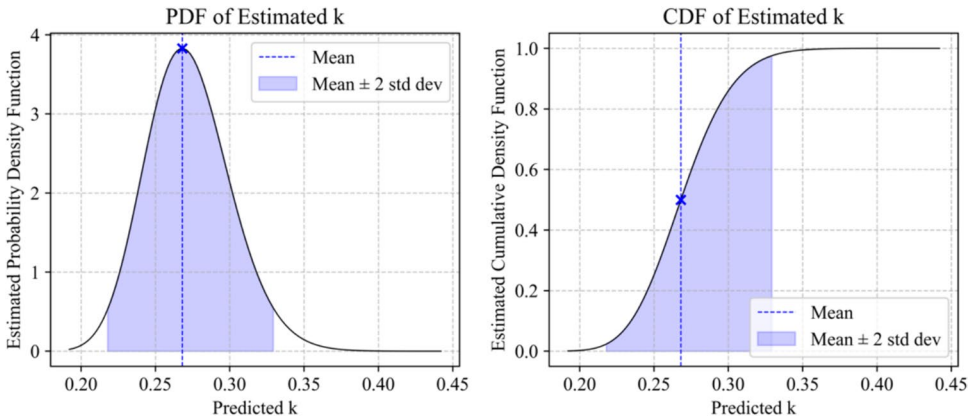

Fig. 10 Probability density function (left) and cumulative density function of predicted TIR, k

improvement rate, even in scenarios with missing or limited data points.

3.5 Material influence on build rate and precision

The layer thickness variability presented in Fig. 6, classified by alloy type, indicates that while material choice significantly impacts manufacturing precision, it does not singularly dictate it. The layer thickness among copper and nickel alloys shows relatively less variance, pointing towards standardization in processing these materials. In contrast, aluminum, steel, and titanium exhibit a broader spread in layer thickness, hinting at the versatility and adaptability of PBF machines to optimize for either speed or precision based on the material in use and the component being produced. The build rates, as demonstrated in Fig. 8, mirror this pattern. The diverse range of build rates for aluminum and steel suggests that PBF machines can be finely tuned to suit specific manufacturing contexts, balancing speed with material properties. The narrower distribution for copper and nickel alloys could indicate a more mature or standardized set of processing parameters for these materials or could indicate material constraints that lower flexibility.

3.6 Technological progress and industry trends

The temporal analysis of build volume and build rate reveals a trajectory toward enhanced capabilities of PBF machines, underscoring the industry's push towards larger and faster manufacturing solutions. This aligns with the growing demand across various sectors. The utilization of PBF in industries like aerospace is rapidly expanding due to its ability to create lightweight metal components that meet strict mechanical and performance standards [87]. PBF is also gaining popularity in the tooling industry for its flexibility in producing optimized forming tools [88]. As researchers and manufacturers continue to push the boundaries of what PBF can achieve, the technology is likely to see increased adoption across various sectors, particularly in aerospace, automotive, and medical industries where the demand for lightweight, high-strength components is driving innovation.

To analyze the build rate trend in PBF, several studies provide valuable insights and aligned results. Wong et al. [26] demonstrated a significant increase in build rate by 2.74 times, resulting in a 63% reduction in build time compared to traditional PBF processes, without compromising mechanical properties. Sing and Yeong [25] support this by concluding that multi-laser PBF exhibits a higher build rate compared to single-laser systems without significantly affecting part density or microstructure. However, Wilson [89] notes that PBF processes generally have slow build rates and limited build volumes when compared to traditional technologies, which can hinder productivity and increase production costs. The challenges related to the lower build rate and productivity of PBF contribute to higher production costs and limited reproducibility, as indicated by Bakhtari [90]. Li et al. [91] mention that the build rate in PBF is typically below 5 mm^3/s but can be increased to 7.2 mm^3/s by adjusting the layer thickness, emphasizing the influence of process parameters on build rate optimization. In the context of industrial success, Abrami et al. [92] stress the importance of achieving high build rates in PBF to manufacture components defect-free and with the desired properties. Furthermore, Letenneur et al. [93] experimentally demonstrated the impact of build rate on surface roughness, showing that adjusting build rates can influence the quality of different parts of the component.

To optimize the production of larger components in PBF, several key factors need to be considered. Wong et al. [26] demonstrated that utilizing multiple lasers can significantly increase the build rate in PBF processes. Adegoke et al. [94] highlighted that finer grain sizes in PBF-manufactured materials can contribute to achieving this goal. In addition, Smith et al. [95] emphasized the successful dispersion of nanoscale oxides throughout the build volume, which is crucial for ensuring structural integrity in larger components. Moreover, optimizing processing parameters, as discussed by Liu et al. [96], is essential to improve the relative density and surface roughness of components fabricated through PBF. Koenis [97] pointed out that preventing local overheating during the PBF process can lead to a more homogeneous temperature distribution, which is vital for building larger components consistently. In terms of material selection, Akilan et al. [98] highlighted the importance of powder characteristics and chemical composition on properties such as corrosion resistance. Understanding the impact of these factors can help in selecting the most suitable materials for building larger components via PBF. To achieve the goal of building larger components in PBF, utilizing multiple lasers, optimizing processing parameters, ensuring material quality, and controlling the build process to prevent issues like overheating are crucial aspects to consider.

4 Conclusions

In this study, we empirically estimated the TIR of PBF technology, which is widely used in aerospace, automotive, and medical industries. We began by conducting a comprehensive literature review to identify the most relevant technical parameters for measuring the capabilities of PBF. Using this information, we established an ideal functional performance metric tailored for PBF technology. Considering all available data sources and every commercially available PBF machine, we constructed a detailed data set of technical parameters. This data set underwent a rigorous data curation

process to ensure data availability and reliability. The resultant practical FPM was then utilized to estimate the TIR of PBF via a regression analysis.

This empirical investigation into the TIR of PBF technology provides a quantitative affirmation of the rapid advancements within the field. By constructing and analyzing a data set that spans over two decades of PBF machine development, we have estimated a robust TIR at 26.8%, showing the technology's potential to further impact industries such as aerospace, automotive, and medical. Our introduction of a Functional Performance Metric for PBF machines has facilitated a nuanced understanding of the technology's evolution. The FPM, informed by an extensive literature review and regression analysis, has proven to be a reliable tool for capturing the essence of technological progression in PBF.

Our study's alignment with the patent-derived improvement rate of 33.3% for PBF–LB/M [80] must be pointed out. This correlation reinforces the credibility of the patent-based TIR method and supports the exponential performance growth models proposed by Moore [69] and further expanded by other researchers [67, 70–75]. Moreover, the convergence of our results with the broader array of improvement rates established through patent analyses across the additive manufacturing spectrum strengthens the argument for the robustness of patent-based approaches.

Overall, our estimated performance improvement underscores the robustness of PBF's growth trajectory. Such insights are invaluable for forecasting future trends, guiding research and development, and aligning investment strategies with the anticipated evolution of the technology. The high estimated yearly rate of improvement, reflective of the PBF technology's advancement, is a testament to the technology's significant role within the additive manufacturing industry. It demonstrates not just a consistent year-over-year improvement but also hints at an emerging impact across industries. As we look towards the future, this TIR serves as a key indicator for industry stakeholders, highlighting PBF's rapid technological advancements and its anticipated influence on manufacturing efficiency, customization, and sustainability.

Despite the metrics' strengths, its limitations must be acknowledged. The data exclusion due to availability and heterogeneity, particularly concerning parameters like surface finish, accuracy, and resolution, could mean that certain aspects of PBF machine performance remain underexplored. In addition, omitting energy consumption and acquisition costs, while necessary due to data constraints, suggests areas for future research. A more comprehensive metric that includes these parameters could provide a holistic view of PBF machines' performance, especially in the context of quality, costs, and sustainability.

In conclusion, the estimated improvement rate aligns with and enhances the body of knowledge established by patent-based studies, offering a concrete metric for comparing and evaluating technological progress in additive manufacturing. It highlights the maturity and innovation potential of PBF, providing a reliable benchmark for the ongoing evolution of additive manufacturing technologies. As PBF technology continues to advance, it is set to contribute to redefining manufacturing paradigms, reinforcing its status as a key technology in industrial applications for years to come.

Supplementary Information The online version contains supplementary material available at https://doi.org/10.1007/s40964-024-00813-8.

Acknowledgements This work has been supported by the European Union under the Next Generation EU, through a grant of the Portuguese Republic's Recovery and Resilience Plan (PRR) Partnership Agreement, within the scope of the project PRODUTECH R3—"Agenda Mobilizadora da Fileira das Tecnologias de Produção para a Reindustrialização", aiming the mobilization of the production technologies industry towards of the reindustrialization of the manufacturing industrial fabric (Project ref. nr. 60—C645808870-00000067; Total project investment: 166.988.013,71 Euros; Total Grant: 97.111.730,27 Euros). Moreover, the authors acknowledge Fundação para a Ciência e a Tecnologia (FCT), through IDMEC, under LAETA, project UIDB/50022/2020.

Funding Open access funding provided by FCT|FCCN (b-on).

Data availability The data used in this research are available for download through the link to the electronic supplementary material provided with the publication. For additional information or inquiries, please contact the corresponding author via institutional email at antonio.campos@tecnico.ulisboa.pt.

References

1. Cordero PM, Mireles J, Ridwan S, Wicker RB (2017) Evaluation of monitoring methods for electron beam melting powder bed fusion additive manufacturing technology. Prog Addit Manuf 2:1–10. https://doi.org/10.1007/s40964-016-0015-6
2. Neil S, Chironis NP (2007) Mechanisms and mechanical devices sourcebook, 4th edn. McGraw-Hill, New York
3. Jayasinghe S, Paoletti P, Sutcliffe C et al (2022) Automatic quality assessments of laser powder bed fusion builds from photodiode sensor measurements. Prog Addit Manuf 7:143–160. https://doi.org/10.1007/s40964-021-00219-w
4. Wohlers Report 2023 reports continued double-digit growth in AM | CompositesWorld. https://www.compositesworld.com/news/

wohlers-report-2023-reports-continued-double-digit-growth-in-am. Accessed 22 Nov 2023
5. Volpato GM, Tetzlaff U, Fredel MC (2022) A comprehensive literature review on laser powder bed fusion of Inconel superalloys. Addit Manuf. https://doi.org/10.1016/j.addma.2022.102871
6. Frazier WE (2014) Metal additive manufacturing: a review. J Mater Eng Perform 23:1917–1928
7. Singh R, Gupta A, Tripathi O et al (2019) Powder bed fusion process in additive manufacturing: an overview. In: Materials Today: Proceedings. Elsevier Ltd, pp 3058–3070
8. DebRoy T, Wei HL, Zuback JS et al (2018) Additive manufacturing of metallic components – process, structure and properties. Prog Mater Sci 92:112–224
9. Murr LE (2015) Metallurgy of additive manufacturing: examples from electron beam melting. Addit Manuf 5:40–53. https://doi.org/10.1016/j.addma.2014.12.002
10. Galati M, Iuliano L (2018) A literature review of powder-based electron beam melting focusing on numerical simulations. Addit Manuf 19:1–20
11. King W, Anderson AT, Ferencz RM et al (2015) Overview of modelling and simulation of metal powder bed fusion process at Lawrence Livermore National Laboratory. Mater Sci Technol (United Kingdom) 31:957–968
12. Yadroitsev I, Yadroitsava I, Du Plessis A, MacDonald E (2021) Fundamentals of laser powder bed fusion of metals, 1st edn. Elsevier, Amsterdam
13. O'Regan P, Prickett P, Setchi R et al (2016) Metal based additive layer manufacturing: variations, correlations and process control. Procedia Comput Sci 96:216–224
14. Baumgartl H, Tomas J, Buettner R, Merkel M (2020) A deep learning-based model for defect detection in laser-powder bed fusion using in-situ thermographic monitoring. Prog Addit Manuf 5:277–285. https://doi.org/10.1007/s40964-019-00108-3
15. Sefene EM (2022) State-of-the-art of selective laser melting process: a comprehensive review. J Manuf Syst 63:250–274
16. Gonçalves A, Ferreira B, Leite M, Ribeiro I (2023) Environmental and economic sustainability impacts of metal additive manufacturing: a study in the industrial machinery and aeronautical sectors. Sustain Prod Consum 42:292–308. https://doi.org/10.1016/j.spc.2023.10.004
17. Caiazzo F, Alfieri V, Corrado G, Argenio P (2017) Laser powder-bed fusion of Inconel 718 to manufacture turbine blades. Int J Adv Manuf Technol 93:4023–4031. https://doi.org/10.1007/s00170-017-0839-3
18. Katz-Demyanetz A, Popov VV, Kovalevsky A et al (2019) Powder-bed additive manufacturing for aerospace application: techniques, metallic and metal/ceramic composite materials and trends. Manuf Rev (Les Ulis). https://doi.org/10.1051/mfreview/2019003
19. Jedlan S, Sevecek M, Prantl A et al (2022) Utilization of additive manufacturing in nuclear power industry. In: 2022 8th international youth conference on energy, IYCE 2022. Institute of Electrical and Electronics Engineers Inc
20. Lin K, Qiao J, Shi K et al (2023) Laser powder bed fusion of micro-channels for the application of proton exchange membrane fuel cell bipolar plates. CIRP J Manuf Sci Technol 43:193–204. https://doi.org/10.1016/j.cirpj.2023.01.007
21. Lowther M, Louth S, Davey A et al (2019) Clinical, industrial, and research perspectives on powder bed fusion additively manufactured metal implants. Addit Manuf 28:565–584. https://doi.org/10.1016/j.addma.2019.05.033
22. Vock S, Klöden B, Kirchner A et al (2019) Powders for powder bed fusion: a review. Pro Addit Manuf 4:383–397
23. Masoomi M, Thompson SM, Shamsaei N (2017) Laser powder bed fusion of Ti-6Al-4V parts: thermal modeling and mechanical implications. Int J Mach Tools Manuf 118–119:73–90. https://doi.org/10.1016/j.ijmachtools.2017.04.007
24. Tsai CY, Cheng CW, Lee AC, Tsai MC (2019) Synchronized multi-spot scanning strategies for the laser powder bed fusion process. Addit Manuf 27:1–7. https://doi.org/10.1016/j.addma.2019.02.009
25. Sing SL, Yeong WY (2020) Laser powder bed fusion for metal additive manufacturing: perspectives on recent developments. Virtual Phys Prototyp 15:359–370
26. Wong H, Dawson K, Ravi GA et al (2019) Multi-laser powder bed fusion benchmarking—initial trials with inconel 625. Int J Adv Manuf Technol 105:2891–2906. https://doi.org/10.1007/s00170-019-04417-3
27. Chen J, Liu Y, She Y et al (2024) The effect of epoxy resin on the infiltration of porous metal parts formed through laser powder bed fusion. J Compos Sci. https://doi.org/10.3390/jcs8030099
28. Lee YS, Zhang W (2016) Modeling of heat transfer, fluid flow and solidification microstructure of nickel-base superalloy fabricated by laser powder bed fusion. Addit Manuf 12:178–188. https://doi.org/10.1016/j.addma.2016.05.003
29. Batalha WC, Batalha RL, Kosiba K et al (2023) Effect of scanning strategy on microstructure and mechanical properties of a biocompatible Ti–35Nb–7Zr–5Ta alloy processed by laser-powder bed fusion. J Mater Res 38:154–164. https://doi.org/10.1557/s43578-022-00735-7
30. Malekipour E, El-Mounayri H (2020) Scanning strategies in the PBF process: a critical review. In: ASME International Mechanical Engineering Congress and Exposition, Proceedings (IMECE). American Society of Mechanical Engineers (ASME)
31. Dai S, Liao H, Zhu H, Zeng X (2021) The mechanism of process parameters influencing the AlSi10Mg side surface quality fabricated via laser powder bed fusion. Rapid Prototyp J 28:514–524. https://doi.org/10.1108/RPJ-11-2020-0266
32. Shi W, Li J, Jing Y et al (2022) Combination of scanning strategies and optimization experiments for laser beam powder bed fusion of Ti-6Al-4V titanium alloys. Appl Sci (Switzerland). https://doi.org/10.3390/app12136653
33. Carrion PE, Soltani-Tehrani A, Phan N, Shamsaei N (2019) Powder recycling effects on the tensile and fatigue behavior of additively manufactured Ti-6Al-4V parts. JOM 71:963–973. https://doi.org/10.1007/s11837-018-3248-7
34. Douglas R, Lancaster R, Jones T et al (2022) The influence of powder reuse on the properties of laser powder bed-fused stainless steel 316L: a review. Adv Eng Mater. https://doi.org/10.1002/adem.202200596
35. Abdelwahed M, Casati R, Larsson A et al (2022) On the recycling of water atomized powder and the effects on properties of L-PBF processed 4130 low-alloy steel. Materials. https://doi.org/10.3390/ma15010336
36. Quinn P, Uí Mhurchadha SM, Lawlor J, Raghavendra R (2022) Development and validation of empirical models to predict metal additively manufactured part density and surface roughness from powder characteristics. Materials. https://doi.org/10.3390/ma15134707
37. Mahmoud D, Magolon M, Boer J et al (2021) Applications of machine learning in process monitoring and controls of l-pbf additive manufacturing: a review. Appl Sci (Switzerland). https://doi.org/10.3390/app112411910
38. Gao F, Macquaire B, Zhang Y, Bellet M (2022) A new localized inverse identification method for high temperature testing under resistive heating: application to the elastic-viscoplastic behaviour of L-PBF processed In718. Strain. https://doi.org/10.1111/str.12409
39. Riipinen T, Metsä-Kortelainen S, Lindroos T et al (2019) Properties of soft magnetic Fe-Co-V alloy produced by laser powder

bed fusion. Rapid Prototyp J 25:699–707. https://doi.org/10.1108/RPJ-06-2018-0136
40. Irrinki H, Nath SD, Alhofors M et al (2019) Microstructures, properties, and applications of laser sintered 17–4PH stainless steel. J Am Ceram Soc 102:5679–5690. https://doi.org/10.1111/jace.16372
41. Kurzynowski T, Pawlak A, Smolina I (2020) The potential of SLM technology for processing magnesium alloys in aerospace industry. Arch Civ Mech Eng. https://doi.org/10.1007/s43452-020-00033-1
42. Wei C, Li L (2021) Recent progress and scientific challenges in multi-material additive manufacturing via laser-based powder bed fusion. Virtual Phys Prototyp 16:347–371
43. Sola A, Defanti S, Mantovani S et al (2020) Technological feasibility of lattice materials by laser-based powder bed fusion of A357.0. 3D Print Addit Manuf 7:1–7. https://doi.org/10.1089/3dp.2019.0119
44. Brown B, Newkirk J, Liou F (2021) Materials absorption of nitrogen during pulsed wave L-PBF of 17–4 PH steel. Materials. https://doi.org/10.3390/ma1403
45. Abedi HR, Hanzaki AZ, Azami M et al (2019) The high temperature flow behavior of additively manufactured Inconel 625 superalloy. Mater Res Express. https://doi.org/10.1088/2053-1591/ab44f6
46. Azami M, Siahsarani A, Hadian A et al (2023) Laser powder bed fusion of Alumina/Fe–Ni ceramic matrix particulate composites impregnated with a polymeric resin. J Market Res 24:3133–3144. https://doi.org/10.1016/j.jmrt.2023.03.181
47. Lane B, Moylan S, Whitenton EP, Ma L (2016) Thermographic measurements of the commercial laser powder bed fusion process at NIST. Rapid Prototyp J 22:778–787
48. Pagani L, Grasso M, Scott PJ, Colosimo BM (2020) Automated layerwise detection of geometrical distortions in laser powder bed fusion. Addit Manuf. https://doi.org/10.1016/j.addma.2020.101435
49. Yadav P, Rigo O, Arvieu C et al (2021) Data treatment of in situ monitoring systems in selective laser melting machines. Adv Eng Mater. https://doi.org/10.1002/adem.202001327
50. Modaresialam M, Roozbahani H, Alizadeh M et al (2022) In-situ monitoring and defect detection of selective laser melting process and impact of process parameters on the quality of fabricated SS 316L. IEEE Access 10:46100–46113. https://doi.org/10.1109/ACCESS.2022.3169509
51. Wang Q, Li J, Nassar AR et al (2021) Model-based feedforward control of part height in directed energy deposition. Materials 14:1–20. https://doi.org/10.3390/ma14020337
52. Yonehara M, Tagami M, Kato C et al (2023) In-situ process monitoring and statistical quantication of powder bed forming and build processes in laser powder bed fusion additive manufacturing. https://doi.org/10.21203/rs.3.rs-3496879/v1
53. Di Egidio G, Morri A, Ceschini L, Tonelli L (2023) High-temperature behavior of the heat-treated and overaged AlSi10Mg alloy produced by laser-based powder bed fusion and comparison with conventional Al–Si–Mg-casting alloys. Adv Eng Mater. https://doi.org/10.1002/adem.202201238
54. Tur E (2023) A comprehensive review on sustainability and environmental impact of laser powder bed fusion additively manufactured as-built Ti-6Al-4V parts. El-Cezeri J Sci Eng 10:612–644
55. Brilhante O, Klaas J (2018) Green city concept and a method to measure green city performance over time applied to fifty cities globally: influence of GDP, population size and energy efficiency. Sustainability (Switzerland). https://doi.org/10.3390/su10062031
56. Garcia-Herrero I, Laso J, Margallo M et al (2017) Incorporating linear programing and life cycle thinking into environmental sustainability decision-making: a case study on anchovy canning industry. Clean Technol Environ Policy 19:1897–1912. https://doi.org/10.1007/s10098-017-1373-6
57. Kardos M, Gabor MR, Cristache N (2019) Green marketing's roles in sustainability and ecopreneurship. Case study: Green packaging's impact on Romanian young consumers' environmental responsibility. Sustainability (Switzerland). https://doi.org/10.3390/su11030873
58. Pernetti R, Galbusera F, Cattenone A et al (2023) Characterizing nanoparticle release patterns of laser powder bed fusion in metal additive manufacturing: first step towards mitigation measures. Ann Work Expo Health 67:252–265. https://doi.org/10.1093/annweh/wxac080
59. Dosi G (1982) Technological paradigms and technological trajectories. Res Policy. https://doi.org/10.1016/0048-7333(93)90041-F
60. Benson CL, Magee CL (2012) A framework for analyzing the underlying inventions that drive technical improvements in a specific technological field. Eng Manag Res 1:p2. https://doi.org/10.5539/emr.v1n1p2
61. Christensen, Clayton M (1997) The Innovator's Dilemma: When New Technologies Cause Great Firms to Fail. Harvard Business School Press, Boston, MA
62. Solow RM (1957) Technical change and the aggregate production function. Rev Econ Stat 39:312–320. https://doi.org/10.2307/1926047
63. Arrow K (1962) The economic implications of learning by doing, the review of economic studies. Rev Econ Stud 29:155–173. https://doi.org/10.2307/2295952
64. Kline SJ, Rosenberg N (1986) An overview of innovation. Eur J Innov Manag 38:275–305. https://doi.org/10.1108/14601069810368485
65. Christensen CM (1992) Exploring the limits of the technology S-curve. Part I: component technologies. Prod Oper Manag. https://doi.org/10.1111/j.1937-5956.1992.tb00001.x
66. Christensen CM (1992) Exploring the limits of the technology S-curve. Part Ii: architectural technologies. Prod Oper Manag 1:358–366. https://doi.org/10.1111/j.1937-5956.1992.tb00002.x
67. Koh H, Magee CL (2006) A functional approach for studying technological progress: application to information technology. Technol Forecast Soc Change 73:1061–1083. https://doi.org/10.1016/j.techfore.2006.06.001
68. Basnet S, Magee CL (2016) Modeling of technological performance trends using design theory. Des Sci 2:e8. https://doi.org/10.1017/dsj.2016.8
69. Moore GE (1965) Cramming more components onto integrated circuits. Electron Magaz 114–117
70. Nordhaus WD (2009) The perils of the learning model for modeling endogenous technological change. National Bureau of Economic Research, Working Paper Series No 14638. https://doi.org/10.3386/w14638
71. Nagy B, Farmer JD, Bui QM, Trancik JE (2013) Statistical basis for predicting technological progress. PLoS ONE. https://doi.org/10.1371/journal.pone.0052669
72. Magee CL, Basnet S, Funk JL, Benson CL (2016) Quantitative empirical trends in technical performance. Technol Forecast Soc Change 104:237–246. https://doi.org/10.1016/j.techfore.2015.12.011
73. Martino J (1971) Examples of technological trend forecasting for research and development planning. Technol Forecast Soc Change 2:247–260. https://doi.org/10.1016/0040-1625(71)90003-5
74. Nordhaus WD (2007) Two centuries of productivity growth in computing. J Econ History 67:128–159. https://doi.org/10.1017/S0022050707000058
75. Koh H, Magee CL (2008) A functional approach for studying technological progress: extension to energy technology. Technol Forecast Soc Change 75:735–758. https://doi.org/10.1016/j.techfore.2007.05.007

76. Sahal D (1979) A theory of progress functions. A I I E Trans 11:23–29. https://doi.org/10.1080/05695557908974396
77. Benson CL, Magee CL (2015) Quantitative determination of technological improvement from patent data. PLoS ONE 10:1–23. https://doi.org/10.1371/journal.pone.0121635
78. Farmer JD, Lafond F (2016) How predictable is technological progress? Res Policy 45:647–665. https://doi.org/10.1016/j.respol.2015.11.001
79. Benson CL (2014) Cross-domain comparison of quantitative technology improvement using patent-derived characteristics. Massachusetts Institute of Technology
80. Benson CL, Triulzi G, Magee CL (2018) Is there a Moore's law for 3D printing? 3D Print Addit Manuf 5:53–62. https://doi.org/10.1089/3dp.2017.0041
81. Alves de Campos A, Henriques E, Magee CL (2022) Technological improvement rates and recent innovation trajectories in automated advanced composites manufacturing technologies: a patent-based analysis. Compos B Eng. https://doi.org/10.1016/j.compositesb.2022.109888
82. Alexander AJ, Mitchell BM (1985) Measuring technological change of heterogeneous products. Technol Forecast Soc Change 27:161–195. https://doi.org/10.1016/0040-1625(85)90058-7
83. Alves de Campos A, Leite M (2023) Latest technological advances and key trends in powder bed fusion: a patent-based analysis. In: Springer professional: advances in production management systems. Production management systems for responsible manufacturing, service, and logistics futures. pp 575–589
84. Calderaro DR, Lacerda DP, Veit DR (2020) Selection of additive manufacturing technologies in productive systems: a decision support model | Seleção de tecnologias de manufatura aditiva em sistemas produtivos: Modelo de apoio à decisão. Gestao e Producao 27
85. Ferreira BT, de Campos AA, Casati R et al (2023) Technological capabilities and sustainability aspects of metal additive manufacturing. Prog Addit Manuf. https://doi.org/10.1007/s40964-023-00534-4
86. Box GEP, Cox DR (1964) An analysis of transformations. J R Stat Soc: Ser B (Methodol) 26:211–252
87. Baldi N, Giorgetti A, Palladino M et al (2023) Study on the Effect of preheating temperatures on melt pool stability in inconel 718 components processed by laser powder bed fusion. Metals (Basel). https://doi.org/10.3390/met13101792
88. Boes J, Röttger A, Theisen W (2020) Processing of X65MoCrWV3–2 cold work tool steel by laser powder bed fusion. Steel Res Int. https://doi.org/10.1002/srin.201900445
89. Meier B, Warchomicka F, Ehgartner D et al (2023) Toward a sustainable laser powder bed fusion of Ti 6Al 4 V: powder reuse and its effects on material properties during a single batch regime. Sustain Mater Technol. https://doi.org/10.1016/j.susmat.2023.e00626
90. Bakhtari AR, Sezer HK, Canyurt OE et al (2024) A review on laser beam shaping application in laser-powder bed fusion. Adv Eng Mater. https://doi.org/10.1002/adem.202302013
91. Li H, Liang X, Li Y, Feng L (2022) Performance of high-layer-thickness ti6al4v fabricated by electron beam powder bed fusion under different accelerating voltage values. Materials 15(5):1878. https://doi.org/10.3390/ma15051878
92. Abrami MB, Tocci M, Gelfi M, Pola A (2022) High temperature mechanical properties of AlMgScZr alloy produced by laser powder bed fusion. Procedia structural integrity. Elsevier B.V, Amsterdam, pp 838–846
93. Letenneur M, Brailovski V, Kreitcberg A et al (2017) Laser powder bed fusion of water-atomized iron-based powders: process optimization. J Manuf Mater Process. https://doi.org/10.3390/jmmp1020023
94. Adegoke O, Andersson J, Brodin H, Pederson R (2020) Review of laser powder bed fusion of gamma-prime-strengthened nickel-based superalloys. Metals (Basel) 10:1–26
95. Smith TM, Thompson AC, Gabb TP et al (2020) Efficient production of a high-performance dispersion strengthened, multi-principal element alloy. Sci Rep. https://doi.org/10.1038/s41598-020-66436-5
96. Liu D, Yue W, Kang J, Wang C (2022) Effect of laser remelting strategy on the forming ability of cemented carbide fabricated by laser powder bed fusion (L-PBF). Materials. https://doi.org/10.3390/ma15072380
97. Koenis TPA, Montero-Sistiaga ML, de Smit MJ, Amsterdam E (2023) Simulation Based Process Optimization Towards Homogeneous Ti6Al4V Components. In: IV International Conference on Simulation for Additive Manufacturing (Sim-AM 2023)
98. Akilan AA, Kumar S, Shaikh MQ et al (2023) Effects of powder characteristics and chemical composition on the properties of 25Cr7Ni stainless steel fabricated by laser-powder bed fusion and evaluation of process simulation. Metals (Basel). https://doi.org/10.3390/met13081476